

1
2
3
4
5
6
7
8
9
10
11
12
13
14
15
16
17
18
19
20
21
22

Beyond N and P: the impact of Ni on crude oil biodegradation

**Obioma K. Mejeha ^{1,2*}, Ian M. Head ¹, Angela Sherry ¹, Clare M. McCann ¹, Peter Leary¹,
D. Martin Jones ¹ and Neil D. Gray ¹**

¹ School of Civil Engineering and Geosciences, Newcastle University, Newcastle upon
Tyne, NE1 7RU, United Kingdom

²Federal University of Technology, P. M. B. 1526, Owerri, Nigeria

*correspondence: obioma.mejeha@futo.edu.ng

Running Title: Nickel impacts on hydrocarbon degradation

Keywords: Biodegradation, Biostimulation, Bioremediation, Crude oil, Nickel

Current addresses of corresponding author:

Obioma K. Mejeha: Department of Microbiology, Federal University of Technology, P. M. B.
1526, Owerri, Nigeria; Phone: +2349035621829; email: obioma.mejeha@futo.edu.ng

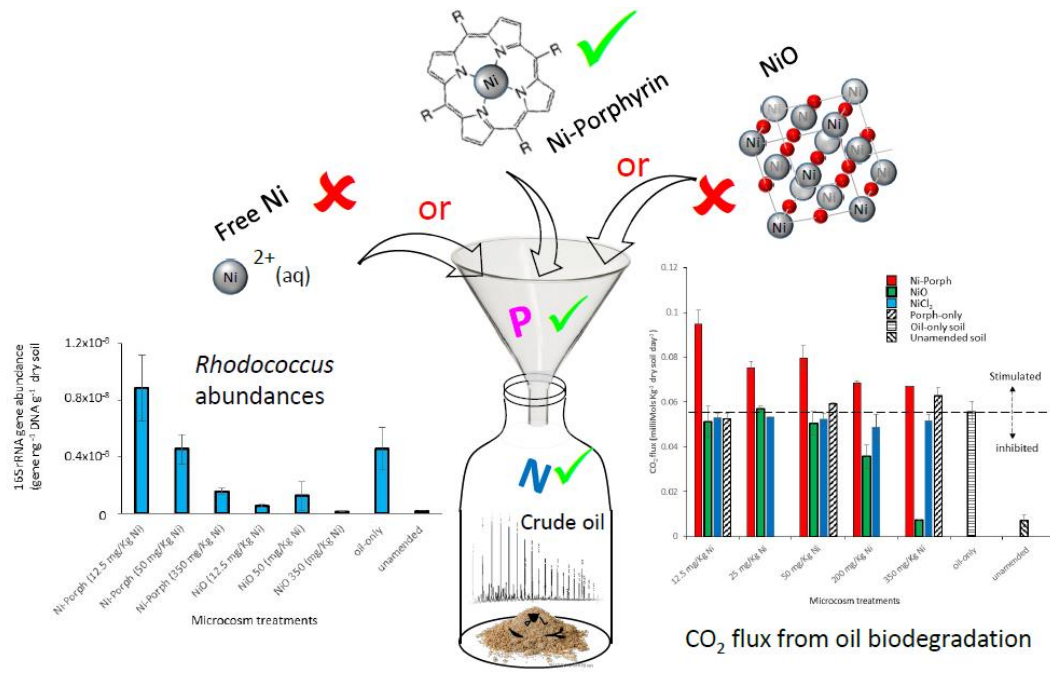
Abstract

N and P are the key limiting nutrients considered most important for the stimulation of crude
oil degradation but other trace nutrients may also be important. Experimental soil

23 microcosms were setup to investigate crude oil degradation in the context of Ni amendments.
24 Amended Nickel as NiO, NiCl₂, or, a porphyrin complex either inhibited, had no effect, or,
25 enhanced aerobic hydrocarbon degradation in an oil-contaminated soil. Biodegradation was
26 significantly (95% confidence) enhanced (70%) with low levels of Ni-Porph (12 mg/Kg)
27 relative to an oil-only control; whereas, NiO (200 and 350 mg/Kg) significantly inhibited (36
28 and 87%) biodegradation consistent with oxide particle induced reactive oxygen stress.
29 Microbial community compositions were also significantly affected by Ni. In 16S rRNA
30 sequence libraries, the enriched hydrocarbon degrading genus, *Rhodococcus*, was partially
31 replaced by a *Nocardia* sp. in the presence of low levels of NiO (12 and 50 mg/Kg). In
32 contrast, the highest relative and absolute *Rhodococcus* abundances were coincident with the
33 maximal rates of oil degradation observed in the Ni-Porph-amended soils. Growth dependent
34 constitutive requirements for Ni-dependent urease or perhaps Ni-dependent superoxide
35 dismutase enzymes (found in *Rhodococcus* genomes) provided a mechanistic explanation for
36 stimulation. These results suggest biostimulation technologies, in addition to N and P, should
37 also consider trace nutrients such as Ni tacitly considered adequately supplied and available
38 in a typical soil.

39 **Highlights**

40 Ni concentration and form added to soil dictated impacts on oil biodegradation
41
42 Biodegradation was enhanced with low concentrations of porphyrin-complexed Ni (12
43 mg/Kg)
44
45 At higher concentrations, Ni oxide but not porphyrin-complexed Ni was inhibitory
46
47 Highest *Rhodococcus* abundances were coincident with porphyrin-complexed Ni stimulation
48



50 **1. Introduction**

51 Despite efforts to find alternative energy sources, oil consumption will continue to increase at
52 least up to 2040 (International Energy Agency, 2015), peaking at over 100 million barrels per
53 day, which is 9–10% higher than the present. With oil spills still occurring in upstream and
54 downstream production activities, there is a continuing need to develop and refine remediation
55 methods for oil contaminated sites. With respect to remediation, the international community
56 now prioritizes the development of methods to protect ecosystems, for instance, the EUs
57 sustainable approach for the remediation of crude oil spills (Kalogerakis et al., 2014).
58 Bioremediation, a process of utilising biological systems to clean up contaminants is
59 considered an efficient, cost effective and eco-friendly approach (Tyagi, et al., 2011) and has
60 been employed for the remediation of major crude oil spills (Atlas and Hazen, 2011; Ron and
61 Rosenberg, 2014).

62 Generally, microbial oil bioremediation is slow relative to more physical and chemical
63 approaches (Macaulay and Rees, 2014). Hence, research studies prioritize improving rates
64 (Macaulay and Rees, 2014) either by manipulating the environment to facilitate rapid
65 proliferation of indigenous hydrocarbon degraders (biostimulation) or by augmentation with
66 non-indigenous hydrocarbon degraders (bioaugmentation) (Tyagi et al., 2011; Nikolopoulou
67 et al., 2013; Suja et al., 2014).

68 For biostimulation, limiting factors such as the concentrations of the main nutrients (nitrogen
69 (N) and phosphorous (P)), are often manipulated to improve biodegradation rates via
70 stimulated enrichment of indigenous aerobic petroleum hydrocarbon degraders (e.g. Singh et
71 al., 2014). Biostimulation has been implemented successfully at number of crude oil
72 contaminated sites. For instance, Inipol EAP22 (an oleophilic fertilizer comprising 7.4% N and
73 0.7% P by weight) and Customblen (a slow nutrient-releasing encapsulated product consisting
74 of 28% N and 3.5% P), enhanced the biodegradation rate of petroleum spilled from the Exxon

75 Valdez in Prince Williams Sound, Alaska, by 5 fold (Tyagi et al., 2011). On a sandy beach at
76 Haifa, Israel, 88% of oil pollutants were removed within 4 months using a nitrogen-enriched
77 culture derived from a polymerized formaldehyde-urea resin mixed with the polymerized
78 nitrogen fertilizer (Ron and Rosenberg, 2014).

79 Additionally, it is well known that trace heavy metals (Co, Cu, Fe, Mn, Mo, Ni, V, and Zn) are
80 required for microbial growth and can stimulate biodegradation activities. For instance,
81 although, excessive amounts of heavy metals become harmful, an absence or low concentration
82 of trace metal is often considered the main factor which limits the anaerobic digestion of
83 organic wastes to biogas (Demirel and Scherer, 2011). As further evidence, the addition of Cu
84 and Fe to a culture of *Rhodococcus jostii* RHA1 enhanced the degradation rate of
85 Tetrabromobisphenol A (Xu et al., 2018) and sub-lethal concentrations of metals (Cu and Cd)
86 have even been shown to stimulate biodegradation of 2-chlorophenol and 3-chlorobenzoate
87 (Kuo and Genthner, 1996).

88 There are indications to suggest that crude oil may contain substantial quantities of metals. For
89 instance, it has been reported that Ni and V can be present in crude oil up to 350 and 1580 ppm,
90 respectively, partly as metalloporphyrins (Filby, 1994). Porphyrins are thought to be derived
91 from phytoplankton or higher plant chlorophylls formed during diagenesis whereby this
92 original complexed magnesium is replaced under specific depositional conditions. Although
93 usually present in trace concentrations (see table S2), oil Ni content in relation to V has led to
94 an oil classification approach based on ratios and absolute concentrations (Barwise, 1990).

95 The aim of this present study was to determine, as an example of a potentially limiting trace
96 metal, the role of Ni as a biostimulant or, potential inhibitor, during petroleum hydrocarbon
97 biodegradation. The effects of different Ni chemical forms, including a porphyrin complex, at
98 different concentrations in soil were assessed. Such studies, for trace metals (akin to those for
99 biostimulation by N and P) when applied to real soils or sediments have not been carried out.

100 Given the typical chemical and physical complexity of such natural systems it is not yet known
101 whether metal additions such as those made to anaerobic digesters or pollutant degrading
102 laboratory cultures are necessary or feasible. For instance, trace nutrients may be adequately
103 supplied by the mineral composition of soils regardless of increased requirements after a spill.
104 Alternatively, the complexity and reactivity of organic matter and mineral phases may rapidly
105 sequester amendments rendering them ineffective.

106 **2. Materials and methods**

107 *2.1. Soil source, physicochemical analysis and microcosm set up*

108 Soil was sourced from a fallow plot under organic management at Newcastle University's
109 Nafferton farm (54°59'08.6"N 1°53'56.2"W) located 24 miles west of Newcastle upon Tyne,
110 UK. This loamy clay soil was classified as a Cambic Stagnogley by the Agrifood Institute
111 (Avery, 1973; Orr et al., 2012) and was considered pristine and suitable for experimental
112 microcosms.

113 Soil pH was determined according to the ISO 10390-2005 Soil quality -- Determination of pH
114 method. The total organic carbon and heavy metal contents of the soils was measured by
115 Derwentside Environmental Testing Services (DETS) Durham, UK according to the Standing
116 Committee of Analysts methods (UK Environment Agency). Soil water holding capacity was
117 determined according to ISO 11274:1998 Soil quality — Determination of the water-retention
118 characteristic.

119 Soil microcosms were set up using sterile 100 ml amber coloured serum bottles closed with
120 rubber septa. Microcosms comprised 10g of air dried and sieved soil (2mm) amended, except
121 for the unamended control, with 100 mg of an undegraded medium gravity North Sea crude
122 oil. Nitrogen (as sodium nitrate) and phosphorous (as potassium dihydrogen phosphate) was
123 added to give a C:N:P ratio of 100:10:1 which was considered sufficient to sustain aerobic

124 microbial growth. Soil moisture contents were adjusted to 60% of the soil water holding
125 capacity to facilitate diffusion of air for aerobic microbial growth in the soil. To understand the
126 effect of Ni on oil biodegradation, triplicate soil microcosm sets were amended with Ni at
127 varying concentrations (12.5, 25, 50, 200 and, 350 mg Ni per kg of dry soil (mg/Kg)) supplied
128 in varying chemical forms (Sigma Aldrich, UK), namely NiO, NiCl₂ and, 5,10,15,20-
129 tetraphenyl-21H,23H-porphine nickel(II) (Ni-porphyrin). Three sets of replicated control
130 microcosms were also prepared which: were not amended with oil or Ni (unamended controls);
131 were amended with oil but not Ni (oil-only controls); amended with oil and Ni-free porphyrin
132 (5,10,15,20-tetraphenyl-21H,23H-porphine) at levels equivalent to that added to the Ni-
133 porphyrin experiments (Ni-free porphyrin controls). All microcosms were incubated at 20°C
134 for 15 days

135 *2.2. Microcosm CO₂ flux rates linked to hydrocarbon degradation*

136 As an oil biodegradation proxy, evolved CO₂ was measured (at 2-day intervals) in headspace
137 gas samples (100 µl) removed using a gas-tight syringe (SGE Analytical, Australia). Analysis
138 was performed using a Fisons MD800 quadrupole mass spectrometer (at 70 eV, filament
139 current 4 A, source current 800 µA, source temperature 200 °C, multiplier voltage 500 V,
140 interface temperature 150 °C) linked to a Fisons 8060 gas chromatograph fitted with an HP-
141 PLOT Q capillary column (30 m X 0.32 m) with 20-µm Q phase and helium as the carrier gas
142 (1ml/min, 65 kPa, split at 100ml/min, 35°C). Peaks (m/z = 44) were calibrated using CO₂ gas
143 standards (Scientific & Technical Gases Ltd, UK). O₂ concentrations (m/z = 32) were
144 simultaneously monitored in microcosm headspaces, which were flushed with air when O₂
145 dropped below 75% of atmospheric levels.

146 *2.3. Residual crude oil (n-alkanes) extraction and analysis*

147 Prior to extraction, 500µg (250µl of a 2000mg / L solution) of a squalane extraction standard

148 representing 0.5% of the added crude oil, was added to soils. Aliquots (10ml) of methanol,
149 toluene and dichloromethane (DCM) were sequentially added to the samples in the microcosm
150 flasks, mixed and vacuum filtered followed by two rounds of rinsing of the residue with the
151 same sequence of solvents. The filtrates were then transferred to a separating funnel with DCM
152 and methanol (30ml of each); deionized water (50 ml) was then added followed by gentle
153 agitation. After settling (1hr), the organic solvent/organic extract phase of the solvent/water
154 mixture was removed. Two additional liquid extraction steps were carried out each by addition
155 of DCM (30 ml) with further agitation. The combined solvent extract was then reduced to ~5ml
156 by rotary evaporation. All microcosm solvent extracts along with aliquots (x3) of the original
157 oil as an undegraded control were then analyzed for total petroleum hydrocarbons. An aliquot
158 of each organic extract or oil was re-suspended in DCM, solvent exchanged into hexane (200 μ l)
159 and added to a 500mg/3ml capacity Isolute®C-18 Solid Phase Extraction (SPE) column
160 (Biotage, UK) and eluted with hexane (5ml) (Bennett et al., 2007). This eluate was reduced in
161 volume, transferred to an autosampler vial made up to 1ml with hexane, together with a known
162 quantity of heptadecylcyclohexane internal standard. The hydrocarbon fraction samples were
163 then injected via a split-splitless injector (held at 300°C) into an HP5890 Series II gas
164 chromatograph (GC) fitted with a flame-ionization detector (FID). The GC was fitted with a
165 30 \times 0.25 mm fused silica capillary column coated with HP-5 phase (0.25 μ m). Hydrogen was
166 used as the carrier gas at a flow rate of 2ml/min. The oven temperature of 50°C was held for 2
167 minutes and then ramped to 300°C at 5°C/min., where it was held for 20min. Data were
168 acquired and processed using Thermo Lab Systems Atlas software to identify n-alkane peaks
169 and quantify their total mass by comparison to the internal standard (n-
170 heptadecylcyclohexane). n-alkane extraction efficiencies were determined from the measured
171 recovery of the added extraction standard (squalane) quantified by reference to the internal
172 standard. Microcosm extraction efficiencies were 88.2 \pm 5.7% (mean \pm SE) and were used to

173 normalize alkane mass values from individual microcosm extracts.

174 *2.4. Microbial community analysis*

175 Soil genomic DNA (~0.25g) was extracted using the PowerSoil ® DNA Isolation Kit (MOBIO
176 Laboratories, USA) in triplicate according to the manufacturer's instructions. The primer set
177 F515/R926 (Quince et al., 2011) was used to polymerase chain reaction (PCR) amplify the
178 variable V4/V5 region of the archaeal and bacterial 16S rRNA gene. F515 was ligated to a
179 PGM™ linker primer/ adapter, a Golay barcode (unique for each sample) and a barcode spacer.
180 R926 was ligated to a truncated P1 (TrP1) adapter at the 5' end (Hamady et al., 2008).
181 Reactions used Bionline's TaqMan DNA amplification kit (Bionline, UK) with conditions of
182 95 °C for 3 minutes followed by 30 cycles (1 min at 95 °C, 45 seconds at 55 °C, 1 minute at
183 72 °C) and finally 10 minutes at 72°C. Amplicons were purified using an Agencourt Ampure
184 XP purification Kit (Beckman Coulter Ltd, UK) and quantified using a Qubit® dsDNA HS
185 Assay Kit (Life Technologies, USA). Amplicons were then pooled into an equimolar library
186 of 500 pM DNA. Sequencing templates were generated by attaching the DNA samples to ion
187 sphere particles using ion PGM™ Template OT2 400 kit (Life Technologies, USA) based on
188 the manufacturer's instruction and using the Ion OneTouch™ 2 Instrument and the Ion
189 OneTouch™ ES. Sequencing was performed using the PGM™ sequencing Platform with the
190 Ion PGM™ sequencing 400 kit followed by filtering to remove low quality and polyclonal
191 sequences. Data was analysed by the Qiime2 pipeline (<https://qiime2.org/>) (Caporaso et al.,
192 2010) to trim and cluster sequences into amplicon sequence variants (ASVs), assign
193 taxonomies and generate representative sequence and ASV frequency outputs. Principal
194 component analysis (PCA) plots were generated from ASV frequencies in the STAMP v2
195 software package (Parks et al., 2014). These plots were generated to provide a two dimensional
196 graphical (exploratory) representation of the variation in community composition.
197 Representative sequences of selected, predominant, ASVs were compared (BLAST) to the

198 NCBI nucleotide database to identify cultured and environmental closely related sequences.
199 Representative 16S rRNA sequence fragments and close relatives were aligned using
200 MUSCLE in MEGA7 to construct a neighbour-joining phylogenetic tree supported by
201 bootstrap analysis (Kumar et al., 2016).

202 2.5. *Quantitative polymerase chain reaction (qPCR)*

203 Bacterial abundances were determined by qPCR using previously developed primer pairs
204 U1048F-U1371R and reaction conditions (Gray et al., 2011). An additional qPCR assay was
205 developed using the PRIMROSE Software (Ashelford et al., 2002) to target the most enriched
206 ASV (genus *Rhodococcus*) in the oil degrading microcosms using RhO1390F (5'-
207 GGTACGGCTACCTTGTTACG-3') and RhO1454R (5'-CACAAGGGGTTAAGCCACCG-
208 3'). The specificity of the qPCR assay was assessed using the RDP probe match analysis tool⁴⁰.
209 The U1048F/U1371R primer pair targeted 90% of all bacterial 16S rRNA sequences (>1200
210 bp), whereas, the RhO1390F/RhO1454R primer pair targeting a small number (128) of
211 sequences classified in the RDP as genus *Rhodococcus* with no non-target matches. The
212 amplicon size of the primer set was 82 bp and the optimum annealing temperature, determined
213 using the thermal gradient facility of the CFX96 Real-Time system (BioRad, UK), was 62 °C.
214 Melt curve analysis was used to determine amplification specificity. qPCR reactions included
215 5 µl of SsoAdvanced™ Universal SYBR® Green Supermix, 0.5 µl of reverse and forward
216 primer (concentration of 10 picomole each), 1 µl of PCR-grade water and 3 µl of template.
217 Reactions included an initial denaturation (7 min at 95°C), followed by 40 cycles of 30 s at
218 95°C, 30 s at 62°C, and 40 s at 72°C. Standards were prepared from a target 16S rRNA
219 sequence cloned from an amplified pure culture of *Rhodococcus erythropolis* (T) DSM 43066).
220 A one-point calibration (OPC) approach (Brankatschk et al., 2012), was used employing
221 individual amplification reaction efficiencies.

222 2.6. Statistical analysis

223 To facilitate the robust statistical analysis of measured variables (i.e., CO₂ flux rates, n-alkanes,
224 and 16s rRNA gene abundances), the experimental design involved replicated experimental
225 soil microcosms randomly assigned into multiple sets of experimental Ni treatment groups (Ni-
226 Porph, NiCl₂, NiO) comprised multiple replicated sub-treatments of different Ni concentrations
227 which were then compared to various controls using one-way analysis of variance (ANOVA).
228 These ANOVA tests were followed, post hoc, by Dunnett's multiple comparison of means
229 which identified which individual sub-treatment mean was different in comparison to a
230 specified single control group mean. For CO₂ flux data and 16S rRNA gene abundance data,
231 comparisons were made both with oil-only and unammended controls. For residual total n-
232 alkanes, comparisons were made with oil-only and undegraded oil controls. The outcome of
233 comparisons are selectively reported in the text as p value thresholds indicative of varying
234 levels of confidence but presented in full table S3. For p values of <0.05, <0.01, and <0.001,
235 means are considered different with 95, 99, and 99.9% confidence, respectively. For p values
236 <0.1, means were considered borderline significantly (i.e., 90% confidence), whereas, those
237 >0.1 were not considered significant. In addition to these hypotheses tests, bivariate correlation
238 analyses was performed on measured rates of hydrocarbon degradation (CO₂ flux rates) and
239 qPCR derived 16S rRNA gene abundance data for the identified hydrocarbon degrading taxon
240 (*Rhodococcus*). Correlation analysis was performed to examine the strength (Pearson
241 correlation coefficient (R)) and significance of the linear relationship between these two
242 variables. All ANOVA and correlation analyses were performed using IBM SPSS statistics
243 version 24.

244

245 3. Results

246 3.1. Soil physicochemical characteristics

247 The soil's pH, total organic matter, water holding capacity and Ni concentrations were,
248 respectively, 7.1 ± 0.03 , $3.1 \pm 0.1\%$ by dry weight, $78.5 \pm 10.7\%$, and 9.1 ± 0.6 mg/kg (i.e., mg
249 Ni per kg of dry soil). The concentrations (mg/kg) of other heavy metals were: Hg, 0.1 ± 0.01 ;
250 As, 11.2 ± 4.4 ; Cd, 0.73 ± 0.1 ; Cr, 17.3 ± 1.5 ; Cu, 15 ± 1 ; Ni, 9.1 ± 0.6 ; Pb, 125.7 ± 71.2 ; Se, < 0.5 ; V,
251 27 ± 3 ; Zn, 81.7 ± 9.9 . Pertinently, the average Ni concentration was below the UK Environment
252 Agency soil guideline value of 130 mg/Kg (Environmental Agency, 2015). All other heavy
253 metals were similarly at low levels.

254 3.2. Effects of Ni on the biodegradation of crude oil in soil microcosms

255 Crude oil biodegradation in replicated soil microcosms was apparent from an approximately
256 linear accumulation of headspace CO₂ over 15 days following oil amendment (see
257 supplementary material, Figure S1). Maximal rates of CO₂ production in Ni and oil amended
258 microcosms relative to oil-only and unamended controls (Figure 1) indicated that oil was
259 readily degraded but the chemical form and concentration of added Ni influenced the rates of
260 degradation. More specifically, amendment with Ni-Porphyrin significantly stimulated CO₂
261 production relative to the oil-only amended control ($p < 0.001$, ANOVA see Table S3).
262 Stimulation was greatest at 12.5 mg/Kg Ni (i.e., the lowest concentration) and progressively
263 reduced with increasing Ni concentration. Maximal rates of CO₂ production (Figure 1) were
264 significantly higher than the oil-only control (Dunnett's comparison of means) at 12.5 mg/Kg
265 Ni ($p < 0.001$) and to a lesser extent at 25 and 50 mg/Kg Ni ($p \leq 0.01$) but not at 200 and 350
266 mg/Kg ($p > 0.1$). This pattern was also found for the final CO₂ yields (see table S4). Ni-free
267 porphyrin amended controls did not show enhanced degradation since the mean CO₂ flux rates
268 from the three different Ni-free porphyrin treatments were not significantly different to the
269 mean rate of the oil-only control ($p > 0.1$, Figure 1, Table S3). Contrary to the Ni-Porphyrin

270 experiments, rates (Figure 1, table S3) and yields (table S4), in NiO and NiCl₂ amended soils
271 were not significantly different at 12-50 mg/Kg relative to the oil-only amended control
272 ($p > 0.1$) and for NiO, there was actually significant inhibition of degradation ($p < 0.01$) at 200
273 and 350 mg/Kg Ni.

274 *3.3. n-Alkane degradation in microcosms*

275 Corroboratory analyses were conducted on residual petroleum hydrocarbons, specifically
276 individual alkanes (n-C₁₁ to n-C₃₂) recovered from treatment microcosms and controls. On the
277 basis of CO₂ flux results, Ni-Porph and NiO at concentrations of 12.5, 50, and 350 mg/Kg Ni
278 were selected for alkane analysis in comparison to the undegraded oil. The undegraded oil prior
279 to degradation contained approximately 8.6% n-alkanes by total oil weight (i.e., $8675 \pm$
280 $718 \mu\text{g}/100 \text{ mg}$ of oil (Figure 2)); whereas, the average total weight of n-alkanes recovered from
281 the different Ni and oil amended soil microcosms ranged from just $828 \pm 619 \mu\text{g}$ for 12.5
282 mg/Kg Ni as Ni- porphyrin to $5203.6 \pm 1651.8 \mu\text{g}$ with 350 mg/Kg Ni as NiO. Total n-alkanes
283 were significantly lower in all the soil microcosm treatments relative to the initial undegraded
284 crude oil ($p < 0.01$) but with less confidence for NiO at 350 mg/Kg ($p < 0.05$) consistent with the
285 CO₂ flux patterns. At 12.5 and 50 mg/Kg Ni as Ni-porphyrin, residual alkanes were apparently
286 lower than in the oil-only controls (Figure 2) although this was not found to be statistically
287 significant (> 0.1). Likewise, at 12.5 and 50 mg/Kg Ni as NiO, the total n-alkane recovered was
288 found to be lower, albeit not significantly, relative to the oil-only amended control.

289 *3.4. Microbial community structure and dynamics in Ni amended and control microcosms*

290 Soil microcosms amended with Ni-Porph and NiO at 12.5, 50, and 350 mg/Kg (i.e., those that
291 were stimulated and inhibited) were used to determine the structure and dynamics of soil
292 microbial communities in relation to controls. The 16S rRNA PCR-DGGE analysis (see
293 supplementary experimental procedures) identified variations in bacterial diversity between

294 different Ni chemical forms and critically, a higher degree of reproducibility between treatment
295 replicates (see supplementary results and discussion and Figure S3). On this basis we reasoned
296 that a 16S rRNA sequence library obtained from the DNA extract of an individual treatment
297 replicate would be broadly representative of the other two replicates. Consequently, 8 barcoded
298 16S rRNA PCR amplicons each from a single but representative treatment replicate were
299 sequenced. The average number of reads in individual binned libraries after filtering was 33806
300 sequences ranging from 23849 to 65672. However, individual libraries were rarefied to 15000
301 for comparative analysis. Sequences have been deposited in the NCBI's Sequence Read
302 Archive (SRA) available under Bio Project PRJNA390800.

303 A principal component analysis (PCA) generated in the STAMP v2 software package (Parks
304 et al., 2014) using ASV frequencies from individual libraries indicated clustering of
305 communities based on Ni-form (Figure 3a). The most abundant ASV in the oil degrading soils
306 was related to the genus *Rhodococcus*, irrespective of Ni form or absence (Figures 3b) and
307 related *Rhodococcus* strains were identified in diverse environments including those that are
308 hydrocarbon-contaminated (Figure 3c). However, the relative abundance of this *Rhodococcus*
309 ASV represented 30, 32, and 28% in the Ni-porphyrin sequence libraries at 12.5, 50, and 350
310 mg/Kg Ni, respectively, whereas it was only 12 and 14% at 12.5 and 50 mg/Kg Ni as NiO.
311 This taxon represented 16% of sequences in the oil-only control but was not enriched at all in
312 the unamended control (0.1%) or with 350 mg/Kg Ni as NiO (0.09%). Thus, porphyrin
313 complexed Ni promoted the proliferation of the *Rhodococcus* whereas the NiO was inhibitory
314 to its growth. A very similar pattern of enrichment, albeit to a lesser extent, was observed for
315 sequences related to the genera *Mycobacterium* and *Pseudomonas* (Figure 3b). In contrast, a
316 *Nocardia* sequence type was most abundant in NiO amended soils at 12.5 and 50 mg/Kg
317 implying the presence of this toxic mineral at moderate levels, selected disproportionately for
318 *Nocardia* growth.

319 In contrast, to the obviously highly enriched and therefore clearly hydrocarbon degrading
320 bacterial taxa such as *Rhodococcus*, the bacterial genera *Bacillus*, *Hyphomicrobium*, and
321 *Bradyrhizobium*, as well as the archaeal family *Nitrososphaeraceae*, were the most abundant
322 taxa in the unamended soil. These typical soil taxa (Figure 3c), were still observable, albeit at
323 a reduced relative abundance, in all the Ni- and oil-amended microcosms. *Nitrososphaeraceae*
324 was the most obviously reduced in relative abundance.

325 3.5. The influence of oil- and Ni-amendment on bacterial and *Rhodococcal* absolute 326 abundances

327 At 12.5 mg/Kg Ni, bacterial 16S rRNA genes in the Ni-porphyrin soil were approximately 3-
328 fold higher, albeit not significantly ($p > 0.1$, table S3), than in the oil-only soils and 9-fold higher
329 ($p < 0.1$) than the unamended controls (Figure 4). At a Ni concentration of 50 mg/Kg,
330 abundances were comparable to the oil-only microcosms; whereas, at 350 mg/Kg Ni
331 abundances were broadly comparable to the unamended control. In all the NiO-amended soils,
332 the mean bacterial 16S rRNA gene abundances were lower, albeit not significantly ($p > 0.1$),
333 than the oil-only soils.

334 Oil-only amendment increased the abundance of *Rhodococcus* by more than an order of
335 magnitude relative to that in the unamended control and this increase was borderline
336 significant (Figure 4, table S3, $p < 0.1$). In the Ni-amended soils, however, abundances of
337 *Rhodococcus* differed based on Ni concentration and Ni-form. In the 12.5 mg/Kg Ni-
338 porphyrin amended oil degrading soil microcosms, the mean abundance of *Rhodococcus* was
339 approximately a third higher, albeit borderline significantly, relative to the oil-only soil (p
340 < 0.1) and approximately 2 orders of magnitude and very significantly higher than the
341 unamended soil ($p < 0.001$). With Ni-porphyrin at 50 mg/Kg the mean *Rhodococcus*
342 abundance was not significantly different relative to the oil-only amended control ($p > 0.1$)
343 but was borderline significantly higher relative to the unamended soil control ($p < 0.1$). In

344 contrast, at a Ni-porphyrin concentration of 350 mg/Kg the *Rhodococcus* abundance was
345 three-fold lower, albeit not significantly ($p > 0.1$), relative to the oil-only amended soil and
346 was not found to be significantly different relative to the unamended soil ($p > 0.1$). In all the
347 NiO-amended soils, *Rhodococcus* abundances were all not significantly different to the
348 unamended controls ($p > 0.1$).

349 Increases in *Rhodococcal* abundances were broadly consistent with their relative enrichment
350 in sequence libraries (Figure 3b), which corroborates the importance of this taxon in oil
351 degradation. Furthermore, bacterial and *Rhodococcal* abundances were strongly correlated
352 with each other ($R = 0.81$; $p < 0.05$) consistent with the finding that, regardless of overall
353 stimulatory or inhibitory effects of Ni on the bacterial community, *Rhodococcus* was the most
354 enriched by oil degradation. For instance, 22.5, 60.5, and 33.4% of the bacterial 16S rRNA
355 gene abundances were accounted for by *Rhodococcus* in the Ni-porphyrin amended soils at
356 12.5, 50, and 350 mg/Kg, respectively. In NiO-amended soils, *Rhodococcal* abundances
357 accounted for 8.8, 18.9, and 2.7% of bacterial abundances at 12.5, 50, and 350 mg/Kg.
358 Furthermore, correlation analysis indicated a strong positive linear relationship between
359 *Rhodococcus* gene abundances and maximal rates of hydrocarbon degradation ($R = 0.86$; p
360 < 0.05).

361 **4. Discussion**

362 Agarry et al., (2013) have previously reported stimulatory effects of low levels of Ni on
363 gasoline degradation in a gasoline-Ni co-contaminated soil. The results presented here,
364 however, provide a broader perspective on this topic and indicate a hitherto overlooked control
365 on hydrocarbon biodegradation dependent, not just on the amounts, but chemical form that
366 metals such as Ni are present or provided in.

367 The organisms enriched in this study were unsurprising since close relatives have been
368 previously identified and/or isolated from oil degrading systems (as evidenced in the
369 phylogenetic tree in Figure 3c) (Pandey et al., 2016). The large genomes of the metabolically
370 versatile *Rhodococcus* typically encode enzymes (monooxygenases, cytochrome P450,
371 dioxygenases, peroxidases, dehydrogenases, acyl-CoA synthase, and fatty acid synthase) for
372 catabolism of alkanes and biosurfactant production. This is certainly the case for the closely
373 related (98% 16S rRNA sequence homology) *Rhodococcus ruber* IEGM 231 (Ivshina and
374 Kuyukina, 2014). A critical question, however, is; why, in the context of Ni amendment, do
375 we see this pattern of hydrocarbon degrader stimulation or inhibition?

376 4.1. The solubility, chemical fate, availability and toxicity of Ni amendments

377 Ni is an essential nutrient required for cell growth and maintenance (Gadd, 2010) but is not
378 thought limiting in culture due to its trace presence in media reagents. Ni in natural
379 environments is more problematic because Ni²⁺ solubility is low; 2 ppb in sea water or 0.3 ppb
380 in fresh water (Eitinger and Mandrand-Berthelot, 2000). In a soil the availability of Ni was
381 found principally dependent on the total Ni content, whereby, added amounts of NiCl₂
382 correlated positively with dissolved Ni concentrations (Zhang et al., 2015). However, at pHs
383 similar to the current study, Ni was rapidly removed from solution via sorption to organic
384 matter, Fe and Al oxides and clay (Zhang et al., 2015). In this current study, the fate of added
385 Ni determined through sequential extraction (see supplementary material) indicated that Ni
386 was not present in an easily exchangeable form.

387 Despite Ni insolubility, artificial (EDTA) or biological (siderophores) chelating agents are a
388 mechanism for solubilising such heavy metals. For instance, the highly efficient assimilation
389 of metalloporphyrins documented for indigenous microorganisms of the Kuperferschiefer
390 black shale, Poland was followed by intracellular degradation of the porphyrin, freeing metal
391 ions within cells (Matlakowska and Sklodowska, 2010). We speculate that porphyrin chelated

392 Ni was more available for uptake and hence more stimulatory to hydrocarbon degradation in
393 our microcosms than similar levels of insoluble NiO or, initially, soluble NiCl₂. Of course, Ni
394 availability, is also dependent on cell uptake requiring regulatory, uptake, chaperone and
395 accessory trafficking proteins (Eitinger and Mandrand-Berthelot, 2000) many of which were
396 ubiquitously observed in 173 *Rhodococcus* genomes searched using the Integrated Microbial
397 Genomes & Microbiomes (IMG/M) system (Markowitz et al., 2012). The alkane oxidising
398 *Rhodococcus ruber* IEGM 231 (Ivshina and Kuyukina, 2014) possessed nixA (a high-affinity
399 nickel-transport protein) and Ni permeases.

400 At high concentrations Ni is toxic (Gadd, 2010); however, suppression levels are likely
401 attributable to the nature and fate of amendments (Nie et al., 2015). For instance, transport via
402 metalloporphyrins is a microbial strategy not only to facilitate metal uptake as discussed above,
403 but also to mitigate intracellular toxic effects Lemire et al., 2013). In contrast, excessive
404 intracellular free metal accumulated from high extracellular Ni²⁺ concentrations or attachment
405 and internalisation of particles (e.g., NiO, Latvala et al., 2016) may result in cell damage.
406 Referring to the previous discussion on the fate of the NiCl₂, its toxicity at higher levels is
407 likely mitigated by the rapid sorption of Ni²⁺ to organic and mineral phases (Zhang et al., 2015)
408 explaining the limited impact of this soluble but un-complexed form relative to the severe
409 impacts of the insoluble NiO powder. With respect to NiO, nanoparticles induce superoxide
410 production and hence reactive oxygen stress (Baek and An, 2011) and supported NiO surfaces
411 promote abiotic superoxide formation during peroxide breakdown (Anpo et al., 1999).
412 Furthermore, NiO cytotoxicity in human epithelial cell lines occurs by the uptake of particles
413 rather than Ni²⁺ with internalisation inducing cytotoxic effects including oxidative stress and
414 DNA damage (Karlsson et al., 2014).

415 *4.2. Impact and putative mechanism of Ni stimulated biodegradation at low levels of*
416 *amendment*

417 At the other end of the Ni concentration range tested, stimulation of oil bioremediation,
418 especially with Ni-porphyrin, suggests Ni was limiting despite the presence of comparable
419 indigenous concentrations. This limitation is interesting because N and P are considered most
420 important during oil bioremediation (Atlas and Hazen, 2011; Coulon et al. 2005). However,
421 in comparable experiments, which investigated the effect of nitrate-N on oil bioremediation in
422 this same, organically managed soil, it is found that nitrogen was not limiting (Mitchell, 2014).
423 Mechanistically, Ni acts as co-factor for 9 enzyme systems (Diekert et al., 1981; Boer et al.,
424 2014). Seven of these are, however, unlikely to stimulate aerobic oil biodegradation and
425 include: glyoxalase 1, responsible for detoxification of methylglyoxal produced during
426 glycolysis; lactase racemase, which catalyses racemization of lactic acids; Ni-Fe hydrogenase,
427 involved in reverse activation of hydrogen in anaerobic (Diekert et al., 1981) and aerobic
428 hydrogen oxidizing systems (Grzeszik et al., 1997); and methyl-coenzyme M reductase
429 involved in anaerobic methane oxidation and methanogenesis (Boer et al., 2014). Ni dependent
430 enzyme are also involved in CO₂ reactions. Carbon-monoxide hydrogenase catalyses the
431 anaerobic oxidation of CO to CO₂ and Acetyl-CoA synthase/decarboxylase anaerobically
432 synthesises acetyl-CoA (Boer et al., 2014). The two remaining Ni associated enzyme systems
433 are more pertinent to aerobic oil biodegradation and are discussed.

434 Ni is a cofactor for urease catalysis of urea to ammonia and carbonic acid (Boer et al., 2014).
435 Interestingly, studies use urease assays to monitor hydrocarbon biodegradation because such
436 activities are highly correlated (Margesin et al., 2000) whereby ammonia release by urease
437 allows growth on organo-nitrogen compounds. However, urease is often 'constitutive': for
438 instance, nitrogen fixing Cyanobacteria regulate significant levels of urease even in the
439 presence of N₂ and NO₃⁻ (Singh, 1992) with urease conforming to a simple growth-rate
440 dependence expression model. Bacterial isolates have indicated that constitutive urease activity
441 is a common trait in soil (Burbank et al., 2012). Most compellingly, levels of soil urease activity

442 directly linked to diesel biodegradation occurred regardless of presence or absence of inorganic
443 (NH_4^+ , NO_3^-) or organic (urea) nitrogen forms (Margesin et al., 2000). It follows, therefore,
444 that hydrocarbon degrader growth likely necessitates uptake of Ni to fulfill constitutive
445 requirements for urease potentially explaining the stimulatory effect of Ni. To support this
446 conclusion, genes coding for urease proteins were ubiquitously identified in *Rhodococcus*
447 genomes.

448 Ni is also, however, a cofactor in superoxide dismutase (SOD) responsible for the
449 detoxification of reactive oxygen species (ROSs) (Lemire et al., 2013). ROSs (i.e., superoxide,
450 hydrogen peroxide, and hydroxyl radicals) are generated by redox active heavy metal
451 contaminants such as Ni but are also by-products of aerobic respiration. Fe-, Mn-, Ni-, and
452 Cu/Zn-containing SOD isoforms catalyse superoxide breakdown into H_2O_2 and O_2 (Fridovich,
453 1997). In combination with catalases (which convert H_2O_2 into H_2O and O_2) SODs, therefore,
454 reduce oxidative stress. It follows that rapid rates of aerobic respiration (indicated in this study
455 by an order of magnitude increase in the CO_2 production from oil) produces a demand for ROS
456 detoxification via superoxide dismutase. Interestingly, in contrast to other SODs, Ni-SODs are
457 primarily found in the bacteria (Fridovich, 1997), specifically, the Cyanobacteria and,
458 intriguingly, the *Actinobacter* (Miller, 2012), which includes the *Rhodococcus* genus. Thus,
459 rapid growth of this hydrocarbon degrader may have necessitated uptake of Ni for Ni-SOD
460 production. However, while Ni-SODs are relatively common in the *Actinobacter* phylum, the
461 *Rhodococcus* genomes survey identified only one Ni-SOD (*Rhodococcus* sp. R04) relative to
462 large numbers of genes for Cu-Zn and Fe-Mn SOD families.

463 **5. Conclusion**

464 Empirically our results indicate a hitherto overlooked limit on hydrocarbon biodegradation
465 dependent on the availability and toxicity of Ni. Explanations (i.e., Ni-dependent urease or

466 super oxide dismutase production) which explain the Ni-stimulated biodegradation patterns
467 observed which will require future work to resolve.

468 More generally the results indicate that, although, biostimulation can be considered an
469 efficient, cost effective and environmentally friendly approach to organic contaminant
470 removal, improvements can be made. Moving beyond provision of N and P, the technology
471 should consider the supply of trace nutrients (i.e. metals) tacitly assumed to be supplied by the
472 environment. Furthermore, it has been demonstrated that the chemical form and fate of the
473 metal and not just its quantity may be important.

474 **Acknowledgements**

475 This work was supported by Petroleum Development trust fund (PTDF) Nigeria and Newcastle
476 University, United Kingdom.

477 **References**

- 478 Avery, B.W., 1973. Soil classification in the soil survey of England and Wales. *J. Soil Sci.*
479 24, 324–338.
- 480 Agarry, S.E., Aremu, M.O., Aworanti, O.A., 2013. Biostimulation and phytoremediation
481 treatment strategies of gasoline-Nickel co-contaminated Soil. *Soil Sediment Contam.* 23,
482 227–244.
- 483 Anpo, M., Che, M., Fubini, B., Garrone, E., 1999. Generation of superoxide ions at oxide
484 surfaces. *Top. Catal.* 8, 189–198.
- 485 Ashelford, K.E., Weightman, A.J., Fry, J.C., 2002. PRIMROSE: a computer program for
486 generating and estimating the phylogenetic range of 16S rRNA oligonucleotide probes
487 and primers in conjunction with the RDP-II database. *Nucleic Acids Res.* 30, 3481–
488 3489.
- 489 Atlas, R.M., Hazen, T.C., 2011. Oil biodegradation and bioremediation: A tale of the two
490 worst spills in U.S. history. *Environ. Sci. Technol.* 45, 6709–6715.
- 491 Baek, Y.-W. and An, Y.-J., 2011. Microbial toxicity of metal oxide nanoparticles (CuO, NiO,
492 ZnO, and Sb₂O₃) to *Escherichia coli*, *Bacillus subtilis* and *Streptococcus aureus*. *Sci.*
493 *Total Environ.* 409, 1603–8.
- 494 Barwise, A.J.G., 1990. Role of nickel and vanadium in petroleum classification. *Energy Fuels*
495 4, 647–652.
- 496 Bennett, B., Noke, K.J., Bowler, B.F.J., Larter, S.R., 2007. The accurate determination of
497 C0–C3 alkylphenol concentrations in crude oils. *Int. J. Environ. Anal. Chem.* 87, 307–
498 320.

- 499 Boer, J. L., Mulrooney, S. B., Hausinger, R. P., 2014. Nickel-dependent metalloenzymes.
500 Arch. Biochem. Biophys. 544, 142–152. doi:10.1016/J.ABB.2013.09.002.
- 501 Brankatschk, R., Bodenhausen, N., Zeyer, J., Burgmann, H., 2012. Simple absolute
502 quantification method correcting for quantitative PCR efficiency variations for microbial
503 community samples. Appl. Environ. Microbiol. 78, 4481–4489.
- 504 Burbank, M.B., Weaver, T.J., Williams, B.C., Crawford, R.L., 2012. Urease activity of
505 ureolytic bacteria isolated from six soils in which calcite was precipitated by indigenous
506 bacteria. Geomicrobiol. J 29, 389–395.
- 507 Caporaso, J.G., Kuczynski, J., Stombaugh, J., Bittinger, K., Bushman, F.D., Costello, E.K.,
508 Fierer, N., Peña, A.G., Goodrich, J.K., Gordon, J.I., Huttley, G.A., Kelley, S.T.,
509 Knights, D., Koenig, J.E., Ley, R.E., Lozupone, C.A., McDonald, D., Muegge, B.D.,
510 Pirrung, M., Reeder, J., Sevinsky, J.R., Turnbaugh, P.J., Walters, W.A., Widmann, J.,
511 Yatsunenko, T., Zaneveld, J., Knight, R., 2010. QIIME allows analysis of high-
512 throughput community sequencing data. Nat. Methods 7, 335–336.
- 513 Coulon, F., Pelletier, E., Gourhant, L., Delille, D., 2005. Effects of nutrient and temperature
514 on degradation of petroleum hydrocarbons in contaminated sub-Antarctic soil.
515 Chemosphere 58, 1439–1448. doi:10.1016/j.chemosphere.2004.10.007.
- 516 Demirel, B., Scherer, P., 2011. Trace element requirements of agricultural biogas digesters
517 during biological conversion of renewable biomass to methane. Biomass Bioenergy 35,
518 992-998
- 519 Diekert, G., Konheiser, U., Piechulla, K., Thauer, R. K., 1981. Nickel requirement and factor
520 F430 content of methanogenic bacteria. J. Bacteriol. 148, 459–464.
- 521 Eitinger, T., Mandrand-Berthelot, M.A., 2000. Nickel transport systems in microorganisms.
522 Arch. Microbiol. 173, 1–9.
- 523 Environmental Agency, 2015. Environment Agency withdrawal of 2009 Nickel SGV 1. 2.
524 doi:10.2903/j.efsa.2015.4002.
- 525 Filby, R.H., 1994. Origin and nature of trace element species in crude oils, bitumens and
526 kerogens: implications for correlation and other geochemical studies. Geol. Soc.
527 London, Spec. Publ. 78, 203–219.
- 528 Fridovich, I., 1997. Superoxide anion radical (O₂⁻), superoxide dismutases, and related
529 matters. J. Biol. Chem. 272, 18515–18517.
- 530 Gadd, G.M., 2010. Metals, minerals and microbes: Geomicrobiology and bioremediation.
531 Microbiology 156, 609–643.
- 532 Gray, N.D., Sherry, A., Grant, R.J., Rowan, A.K., Hubert, C.R.J., Callbeck, C.M., Aitken,
533 C.M., Jones, D.M., Adams, J.J., Larter, S.R., Head, I.M., 2011. The quantitative
534 significance of Syntrophaceae and syntrophic partnerships in methanogenic degradation
535 of crude oil alkanes. Environ. Microbiol. 13, 2957–2975.
- 536 Grzeszik, C., Lubbers, M., Reh, M., Schlegel, H.G., 1997. Genes encoding the NAD-
537 reducing hydrogenase of *Rhodococcus opacus* MR11. Microbiology 143, 1271–1286.
- 538 Hamady, M., Walker, J.J., Harris, J.K., Gold, N.J., Knight, R., 2008. Error-correcting
539 barcoded primers for pyrosequencing hundreds of samples in multiplex. Nat. Methods 5,
540 235–237.
- 541 International Energy Agency, 2015. World Energy Outlook 2015 Factsheet.

- 542 Ivshina, I.B., Kuyukina, M.S., 2014. Draft Genome Sequence of Propane- and Butane-
543 Oxidizing Actinobacterium *Rhodococcus ruber* IEGM 231. *ASM - Genome Announc.* 2,
544 2–3.
- 545 Kalogerakis, N., Nikolopoulou, M., Coivini, P.F.X., Aulenta, F., 2014. Recent advances of
546 EU's FP7 project killspill - Integrated biotechnological solutions for combating marine
547 oil spills. in *Proceedings of the 37th AMOP Technical Seminar on Environmental*
548 *Contamination and Response (Environment Canada)*, 455–467.
- 549 Karlsson, H.L., Gliga, A.R., Calleja, F.M.G.R., Goncalves, C.S., Wallinder, I.O., Vrieling,
550 H., Fadeel, B., Hendriks, G., 2014. Mechanism-based genotoxicity screening of metal
551 oxide nanoparticles using the ToxTracker panel of reported cell lines. *Part. Fibre Toxic.*
552 11, 41–54.
- 553 Kumar, S., Stecher, G., Tamura, K., 2016. MEGA7: Molecular Evolutionary Genetics
554 Analysis Version 7.0 for Bigger Datasets. *Mol. Biol. Evol.* 33, 1870–1874.
- 555 Kuo, C.W., Genthner, B.R.S., 1996. Effect of added heavy metal ions on biotransformation
556 and biodegradation of 2-chlorophenol and 3-chlorobenzoate in anaerobic bacterial
557 consortia. *Appl. Environ. Microbiol.* 62, 2317–2323
- 558 Latvala, S., Hedberg, J., Di Bucchianico, S., Moller, L., Odnevall Wallinder, I., Elihn, K.,
559 Karlsson, H.L., 2016. Nickel release, ROS generation and toxicity of Ni and NiO micro-
560 and nanoparticle. *PLoS One* 11, e0159684.
- 561 Lemire, J.A, Harrison, J.J., Turner, R.J., 2013. Antimicrobial activity of metals: mechanisms,
562 molecular targets and applications. *Nat. Rev. Microbiol.* 11, 371–84.
- 563 Margesin, R., Zimmerbauer, A., Schinner, F., 2000. Monitoring of bioremediation by soil
564 biological activities. *Chemosphere* 40, 339–346.
- 565 Markowitz, V.M., Chen, I.-M.A., Palaniappan, K., Chu, K., Szeto, E., Grechkin, Y., Ratner,
566 A., Jacob, B., Huang, J., Williams, P., Huntemann, M., Anderson, I., Mavromatis, K.,
567 Ivanova, N.N., Kyrpides, N.C., 2012. IMG: Integrated microbial genomes database and
568 comparative analysis system. *Nucleic Acids Res.* 40, D115–D122.
- 569 Matlakowska, R., Sklodowska, A., 2010. Uptake and degradation of copper and cobalt
570 porphyrins by indigenous microorganisms of Kupferschiefer (Fore-Sudetic Monocline,
571 Poland). *Hydrometallurgy* 104, 501-505.
- 572 Miller, A.-F., 2012. Superoxide dismutases: Ancient enzymes and new insights. *FEBS Lett.*
573 586, 585–595.
- 574 Macaulay, M.B., Rees, D., 2014. Bioremediation of oil spills: a review of challenges for
575 research advancement. *Ann. Environ. Sci.* 8, 9–37.
- 576 Mitchell, T.B., 2014. The effect of nutrient kinetics on bioremediation of hydrocarbon
577 contaminated agricultural soil. Newcastle University MSc dissertation thesis.
- 578 Nie, J., Pan, Y., Shi, J., Gua, Y., Yan, Z., Duan, X., Xu, M., 2015. A comparative study on
579 the uptake and toxicity of nickel added in the form of different salts to maize seedlings.
580 *Int. J. Environ. Res. Public Health* 12, 15075–15087.
- 581 Nikolopoulou, M., Pasadakis, N., Kalogerakis, N., 2013. Evaluation of autochthonous
582 bioaugmentation and biostimulation during microcosm-simulated oil spills. *Mar. Pollut.*
583 *Bull.* 72, 165–173.
- 584 Orr, C.H., Leifert, C., Cummings, S.P., Cooper, J.M., 2012. Impacts of organic and
585 conventional crop management on diversity and activity of free-living nitrogen fixing

586 bacteria and total bacteria are subsidiary to temporal effects. PLoS One 7.
587 Pandey, P., Pathak, H., Dave, S., 2016. Microbial ecology of hydrocarbon degradation in the
588 soil: a review. Res. J. Env. Toxicol. 10, 1-15.

589 Parks, D.H., Tyson, G.W., Hugenholtz, P., Beiko, R.G., 2014. STAMP: statistical analysis of
590 taxonomic and functional profiles. Bioinformatics 30, 3123–3124.

591 Quince, C., Lanzen, A., Davenport, R. J., Turnbaugh, P. J., 2011. Removing noise from
592 pyrosequenced amplicons. BMC Bioinformatics 12, 38.

593 Ron, E.Z., Rosenberg, E., 2014. Enhanced bioremediation of oil spills in the sea. Curr. Opin.
594 Biotechnol. 27, 191–194.

595 Singh, A.K., Sherry, A., Gray, N.D., Jones, D.M., Bowler, B.F.J., Head, I.M., 2014. Kinetic
596 parameters for nutrient enhanced crude oil biodegradation in intertidal marine
597 sediments. Front. Microbiol. 5, doi:10.3389/fmicb.2014.00160.

598 Singh, S., 1992. Regulation of urease cellular levels in the cyanobacteria *Anacystis nidulans*
599 and *Nostoc muscorum*. Biochem und Physiol der Pflanz 188, 33–38.

600 Suja, F., Rahim, F., Taha, M.R., Hambali, N., Rizal Razali, M., Khalid, A., Hamzah, A.,
601 2014. Effects of local microbial bioaugmentation and biostimulation on the
602 bioremediation of total petroleum hydrocarbons (TPH) in crude oil contaminated soil
603 based on laboratory and field observations. Int. Biodeterior. Biodegrad. 90, 115–122.

604 Tyagi, M., da Fonseca, M.M.R., de Carvalho, C.C.C.R., 2011. Bioaugmentation and
605 biostimulation strategies to improve the effectiveness of bioremediation processes.
606 Biodegradation 22, 231–241.

607 Xu, S., Wang, Y-F., Yang, L-Y., Ji, R., Miao, A.J., 2018. Transformation of
608 tetrabromobisphenol A by *Rhodococcus jostii* RHA1: Effects of heavy metals.
609 Chemosphere 196, 206-213.

610 Zhang, X., Li, J., Wei, D., Li, B., Ma, Y., 2015. Predicting Soluble Nickel in Soils using Soil
611 Properties and Total Nickel. PLoS One 10, e0133920.

612

613 **Figure Legends**

614 Figure 1. A) Maximal rates of CO₂ production in: Ni- and oil-amended soils; Ni-free porphyrin
615 and oil amended soils; oil-only and; unamended-controls. The horizontal dotted line indicates,
616 for comparison, the maximal mean CO₂ production rate of the oil-only control. Treatments
617 with rates above or below the dotted line are considered stimulatory or inhibitory, respectively.
618 The x-axis indicates microcosm added Ni- or equivalent porphyrin concentration. Each bar
619 represents the mean maximal rate (n=3). Error bars represent 1 x standard error.

620 Figure 2: Mass of n-alkanes recovered after 15-day incubations of replicated soil microcosms
621 amended with oil (100 mg) and different quantities and types of Ni in comparison to the mass

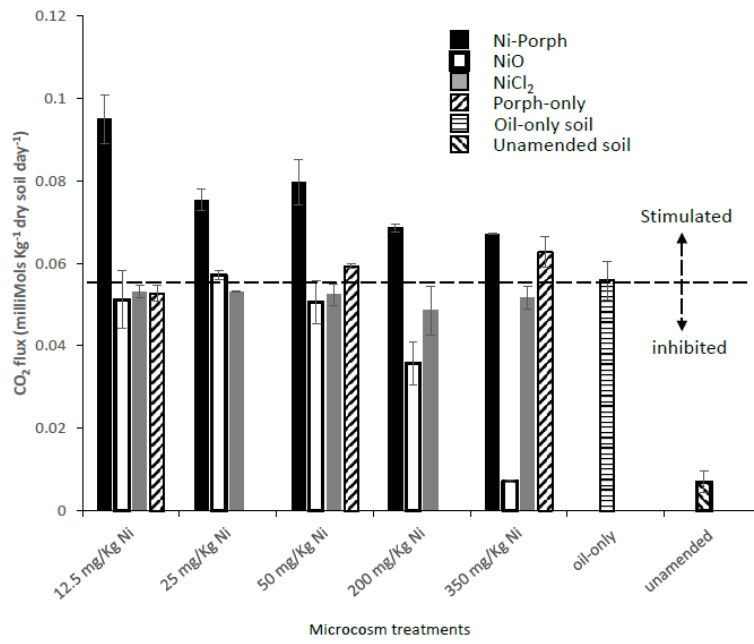
622 of alkanes recovered from the oil-only amended controls. For comparison the n-alkane content
623 of replicated 100 mg aliquots of fresh undegraded crude oil are also shown. Error bars represent
624 1 x the standard error (n=3).

625 Figure 3. (A) Principal Component Analysis (PCA) of 16S rRNA sequence libraries from
626 representative Ni-oil amended, oil-only, and unamended soil microcosms. (B) Fractional
627 abundances of selected dominant taxa in 16S rRNA sequence libraries representative of Ni-oil
628 amended, oil-only and unamended soil microcosms. (C) Phylogenetic distance tree
629 (Neighbour-Joining) of selected dominant bacterial and archaeal taxa identified in microcosm
630 sequence libraries and their close relatives. The tree is based on a comparative analysis of
631 selected partial 16S rRNA sequences and taxa identified in this study are indicated by
632 individual codes assigned during pipeline analysis. The percentage of replicate trees in which
633 the associated taxa clustered together in bootstrap analysis (1000 replicates) are shown next to
634 the branches.

635 Figure 4: Absolute abundances of bacterial and *Rhodococcus* 16S rRNA genes in soil
636 microcosms after 15 days incubation. Each bar represents the mean 16S rRNA gene abundance
637 (in genes ng^{-1} DNA g^{-1} soil) from triplicate samples. Error bars = 1 x the standard error.

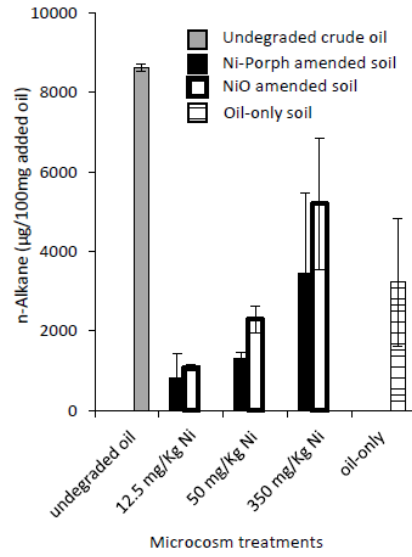
638

Mejeha et al. figure 1



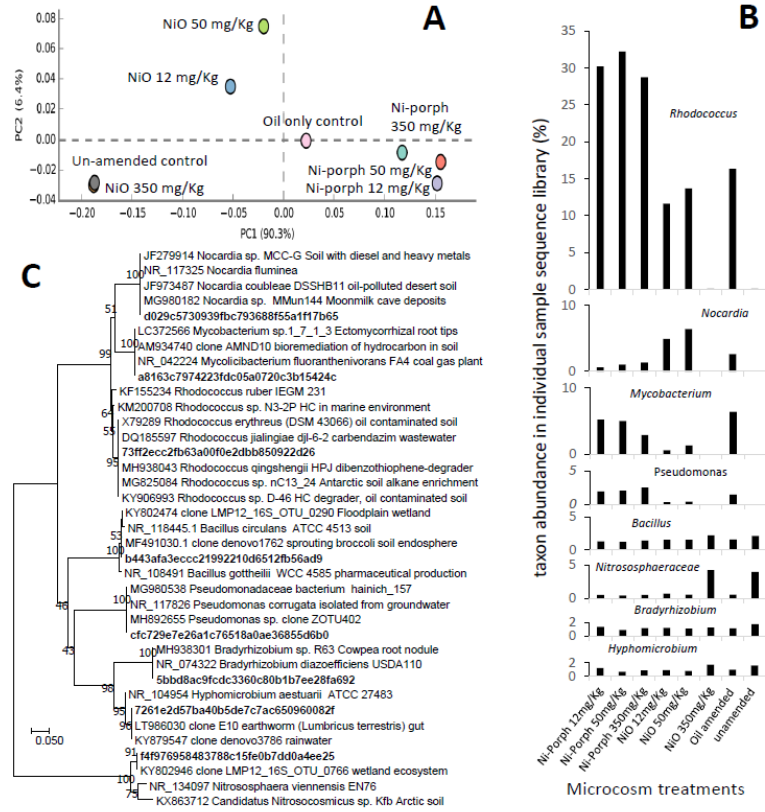
639

Mejeha et al. figure 2



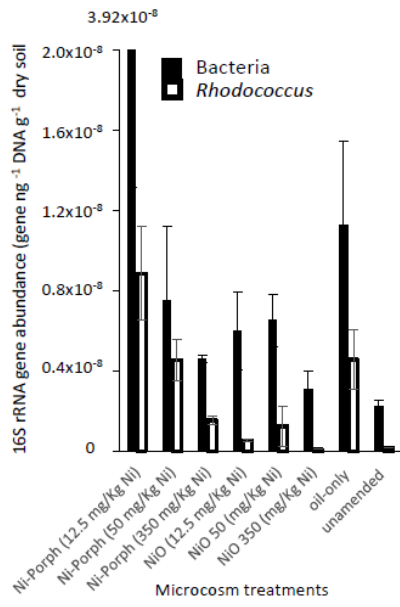
640

Mejeha et al. figure 3



641

MeJeha et al. figure 4



642